World Academy of Science, Engineering and Technology
International Journal of Geotechnical and Geological Engineering
Vol:11, No:9, 2017

Experimental Simulation of Soil Boundary Condition for Dynamic Studies

Omar.S. Qaftan, T. T. Sabbagh

***Abstract*—**This paper studies the free-field response by adopting a flexible membrane container as soil boundary for experimental shaking table tests. The influence of the soil container boundary on the soil behaviour and the dynamic soil properties under seismic effect were examined. A flexible container with 1/50 scale factor was adopted in the experimental tests, including construction, instrumentation, and determination of the results of dynamic tests on a shaking table. Horizontal face displacements and accelerations were analysed to determine the influence of the container boundary on the performance of the soil. The outputs results show that the flexible boundary container allows more displacement and larger accelerations. The soil in a rigid wall container cannot deform as similar as the soil in the real field does. Therefore, the response of flexible container tested is believed to be more reliable for soil boundary than that in the rigid container.

***Keywords*—**Soil, boundary, seismic, earthquake, ground motion.

I. Introduction

THE soil boundary condition is a simulation condition, which represents the accuracy of the experimental test output. In reality, the soil is unbounded. However, the effect of the soil boundary is required to be studied due to the influence boundary on the behaviour of soil during experimental tests. In the shaking table experiments, the container influences soil behaviour of SFSI system due to wave reflection on the container boundary and variation of system vibration mode. A suitable simulation of soil boundary is necessary to enable the soil in the container to get the same deformation as the soil prototype and to minimise the impact of boundary condition. Many researchers proposed different kinds of soil container to simulate the boundary conditions of dynamic soil tests. The main available studied container is laminar box, winged wall box, generally rigid wall box with inner lining, and the flexible container. The region near the boundary is more affected by the boundary condition in comparison with the area far from the boundary. It is found that the ratio D/d should be taken as 5 by controlling the size of the structure plan, where (D) and (d) is the diameter of the soil container and the structure base diameter, respectively [9].

II. Dynamic Behaviours of Soil

The response of soils to dynamic loads is controlled mostly by the soil mechanical properties of soil. The soil mechanical properties associated with dynamic loading are shear wave velocity (V_s), shear modulus (G), the damping ratio (D), and Poisson's ratio (ν). Wave propagation effects control the engineering problems. These effects induce low levels of strain in the soil mass. However, when soils are subjected to dynamic loading that may cause a stability problem, then considerable strains are induced. References [9], [16] show the hysteresis soil behavior when the soil under dynamic load. This hysteresis response of soils can be estimated by considering two important parameters of hysteresis loop shape [7], [3], [5] the loop inclination represents the stiffness, the tangent shear modulus varies with the dynamic loading. However, the average value of the loop entirely can be estimated approximately by the secant shear modulus (G_{sec}) (1), where the τ_c and γ_c are the shear stress and shear strain, respectively.

$$G_{sec}=\frac{\tau_c}{\gamma_c} \quad (1)$$

Therefore, G_{sec} describes the general inclination of the hysteresis loop. If the result of the damping ratio (D) is less than 1, the damping ratio is defined as under damping, while if those values are equal to 1 and more, the damping ratio is defined as critical damping and over damped, respectively. Most problems in earthquake engineering are within underdamped limits. The damping ratio represents the ability of material to dissipate dynamic load or dampen the system. It should be noted that many parameters affect the stiffness of soils during dynamic loadings, such as relative density, plasticity index, main principal effective stress, over consolidation ratio, the number of load cycles and void ratio.

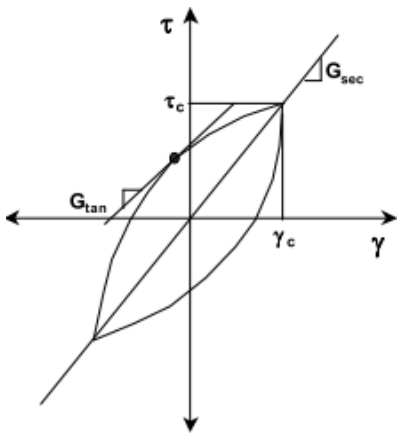

(a) Hysteresis loop

F.A.Omar.S.Qaftan (postgraduate researcher (PhD Student)) is with the Civil Engineering Department, University of Salford, The crescent, M5 4WT, U.K, (corresponding author, phone: +44(0)7440431108, e-mail: o.s.s.sadq@edu.salford.ac.uk).

S. B. Dr Tahsin **Toma** Sabbagh (Lecturer) is with the Civil Engineering Department, University of Salford, The Crescent, M5 4WT, U.K (e-mail: t.toma@salford.ac.uk.).

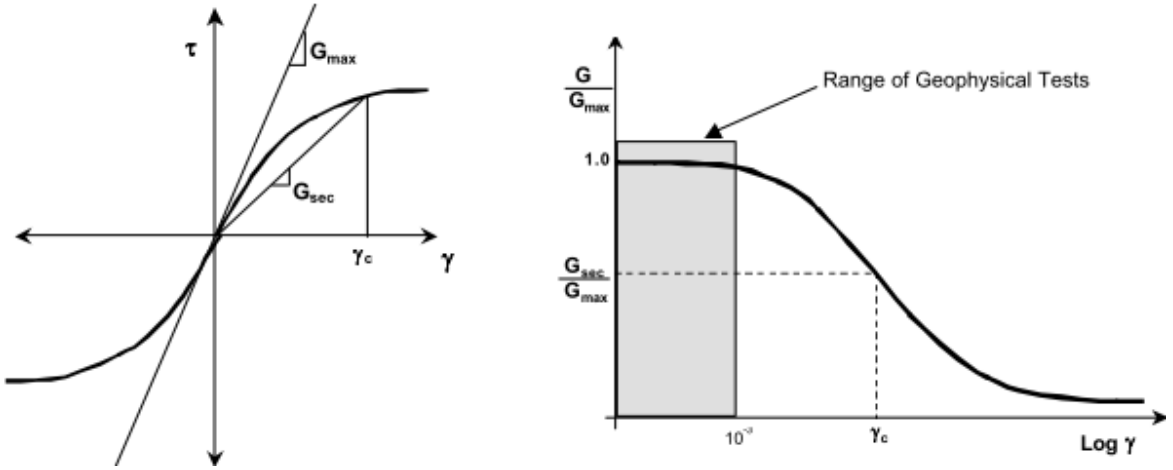

(b) Secant and tangent shear modulus

Fig. 1 (a), (b) Hysteresis loop showing secant and tangent shear modulus due to the strain amplitude variation [5], [13]

Fig. 1 (a) shows the loss of soil element stiffness with an amplitude of strain. The damping force increases and causes the energy dissipated in the ground by friction, heat, or plastic yielding. Damping or the damping ratio (D) is defined as the damping coefficient divided by the critical damping coefficient. The damping (D) can be estimated from the hysteresis loop, the area of the loop divided by the triangle area created by the secant modulus and the maximum strain (energy dissipated in one cycle of the peak energy during a load cycle), see Fig. 1 (b).

$$\zeta = \frac{w_D}{4\pi w_s} = \frac{1}{2\pi} \frac{A_{loop}}{G_{sec}\gamma c^2} \frac{\tau_c}{\gamma_c} \quad (2)$$

The indication of the low-strain soil models is based on the approach of the equivalent linear model. This method is simple and used in a dynamic model commonly, but they have a limited ability to represent many aspects of soil behaviour under dynamic loading conditions.

III. Boundary Conditions of the Ground Free-Field

The boundary conditions reviewed and designed to absorb the reflection of the outgoing waves. They can be used without any additional modification when the source of excitation is within the model. During the excitation or when the reflected seismic waves are incoming, the absorbing boundary conditions (ABCs) of the experimental model need to extend.

Along the surrounding area of the model, the motion is not known. Reference [19] described a method called free-field soil columns. The soil columns are solved in parallel with the main model. The free-field motions are converted into boundary tractions, which are applied directly to the model [10].

IV. Testing Platform

References [9], [13] summarized the different analysis outputs on soil container analysis. The QUAD4M software for the 40ft deep deposit of San Francisco Bay Mud was used as a case study. This test was carried on three different kinds of the container (rigid wall box, wing wall box, and flexible wall box). This analysis demonstrated the advantage of a flexible container over rigid-wall designs in replicating the prototype response. Reference [9] concluded two issue. Firstly, the flexible container and the relevant constructional details should be conducted properly to minimise the box effect. Secondly, the container diameter should be 5 times greater than the structure width. The flexible container adopted in this study has 1-meter diameter width and one-meter depth. The first year up to the mid of the second year of this project was spent in acquiring the required materials, modifying and fabricating the testing instruments. To perform a scale model test on the shake table, the scaling of critical variables like dynamic soil strength, dynamic structural response, and seismic displacements need to be similar. The similitude analysis procedure was clarified in details by [8]. The main piece of testing equipment is a 5-mm flexible membrane wall that represents the response of free-field seismic site when the model is subjected to excitation of the shake table. Validation of the testing platform involves in comparing the analytical results with the recorded response of the flexible wall barrel. Reference [8] shows the validation and demonstration of the dynamic performance of the flexible barrel versus other the types of testing containers. He concluded that the flexible wall barrel provides the most accurate representation of seismic soil response in comparison with the prototype soil column as modelled numerically using QUAD4M [8].

V. Container Construction and Testing Procedure

[14]Moreover, [2] describes single-axis flexible containers for 1-G seismic tests on shaking tables. Single-axis flexible containers permit movement in a single axis only and typically comprise either rigid guide walls that support laminae on bearings or laminae that are stacked on each other separated by bearings in addition to single-axis containers [8], [9]. Moreover, they provide details of double-axis flexible containers for 1-G tests. Double-axis containers permit horizontal movement of laminae in two principal directions.

The container comprises a ribbed membrane hanging from a top ring and it is supported by a frame using universal joints. An improved fixable container was adopted in this study and the container details and the testing procedure are clarified as follows:

A. Experimental Set-Up

The flexible container was designed and manufactured at the University of Salford. Fig. 3 shows the flexible container, which consists of 5-mm membrane cylinder wall supported individually by stiffener strips. The top ring is fixed by lifting hooks which are supported by lifting crane. The bottom base is set on the shaking table.

Fig. 2 Soil Container Fixed on Shaking Table at Salford University

B. Soil Properties and Placement

The dry sand was used as the backfill material. This sand has sub-rounded particles; Fig. 4 and Table I show the grain size distribution of the sand. The selected sand is classified as a poorly graded sand (SP) by adopting The Unified Soil Classification System. The maximum dry density of the sand is 15.5 kN/m^3 in a vibration test and a minimum dry density of 14.5 kN/m^3. The specific gravity of the chosen sand is 2.68, and the other properties are shown in Table I. The friction angle was measured as 36 ° in direct shear tests; sand was placed in the container using the eluviation (raining) technique to achieve uniform density. The actual relative densities were achieved and measured by collecting samples in small cups with known volume placed at different locations.

The maximum shear modulus for the deposit is calculated by using an empirically derived relationship for sands [5]:

$$G_o(\mathrm{d}) = \frac{\mathbf{3230}\,(2.973-e)^2\sqrt{\sigma_m'}}{\mathbf{1+e}} \quad (3)$$

where σ_m' is the main effective confining stress. [5] measured K0 values of 0.445 and 0.46 for dense and loose sand. At the base of the shear stack, K0 is assumed as 0.45 (the average of Stroud's measurements), σ'_m is calculated as 4.5 kN/m^2 rendering G0 at the same location as 34 MPa.

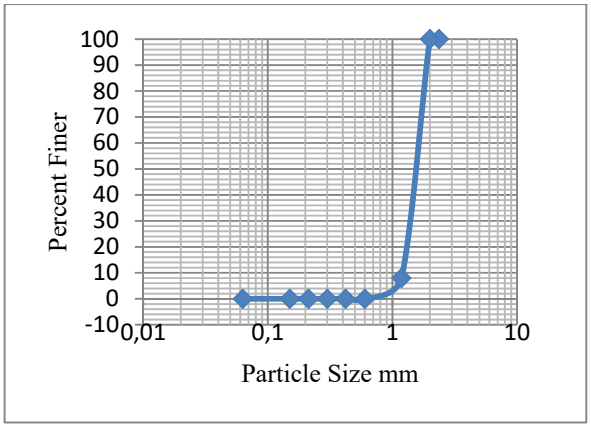

Fig. 3 Selected Soil

TABLE I
PROPERTIES OF THE TEST SAND

Symbol	Quantity	Value
D10mm	Effective size	1.3
D30mm	Effective size	1.5
D50 mm	Mean grain size	1.7
D60 mm	Mean grain size	1.8
D mm	Particle size range mm	0.6 – 1.18
Cu	*Coefficient of uniformity*	1.38
Cc	*Coefficient of curvature*	0.96
	Soil classification	SP
	Soil Description	Poorly graded sand
γ	*Max. Dry unit weight*	15.5 kN/m^3
γ	*Min. dry unit weight*	14.5kN/m^3
e_{max}	*Max. Void ratio*	0.48
e_{min}	*Min. Void ratio*	0.6

m = meter, kN = kilonewton.

C. Accelerogram Generation

By using some special software (Seismo Artif), four-time history events were generated with different peak ground acceleration (0.05 g, 0.1 g, 0.15 g, 0.2 g), see Fig. 5. These events are complying with Euro Code EC8 and were adopted for as dynamic load inputs.

D. Tests Performed and Instrumentation Details

Fig. 6 shows a cross-section of the flexible container with the instrumentation layout. A total of six accelerometers (ACC1–ACC6). Three of the accelerometers were mounted on the soil surface. Accelerometers ACC2–ACC3 were situated along the longitudinal axis of the soil layer. ACC5 was located on the horizontal axis of the sand layer offset 50 mm from the top surface. ACC6 was embedded at the mid-height of the soil column directly above ACC1. The effects of container boundaries were investigated; a small amplitude (0.1 g) harmonic excitation was applied to the shaking table and flexible container to ensure linear soil behavior. Since ACC1–ACC6 inclusive are most accurate at frequencies of 3 Hz and higher, sinusoidal waves were generated at 0.1 g.

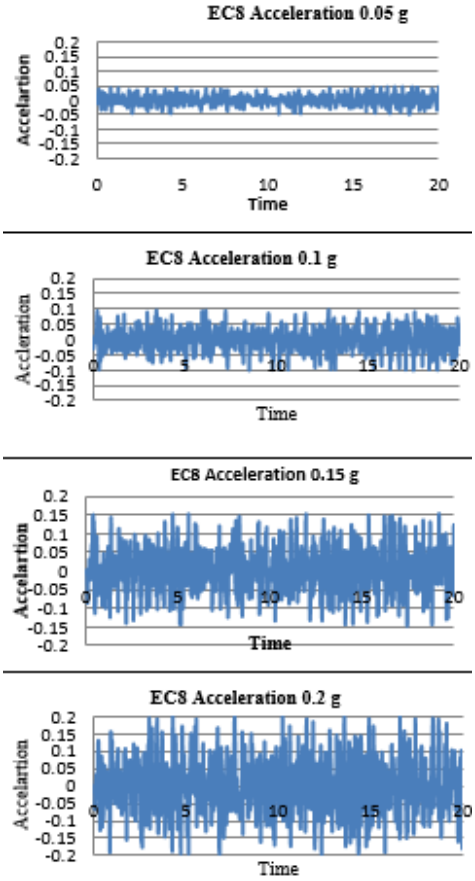

Fig. 4 Acceleration input data

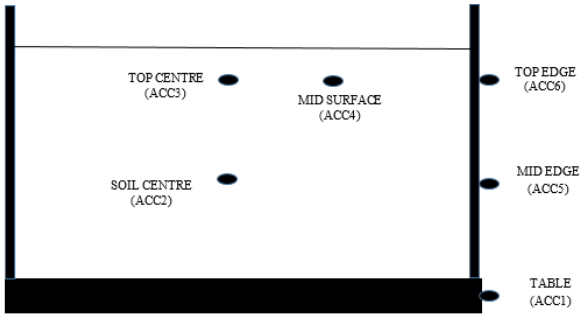

Fig. 5 Acceleration layout

VI. Interpretation of Experimental Data

Interpretation of ground motion amplification of the soil container was conducted using (4):

$$\rho_{amp}=\frac{\boldsymbol{max}(|\ddot{x}_{\boldsymbol{soil}}(\boldsymbol{t})|)}{\boldsymbol{max}(|\ddot{x}_{\boldsymbol{table}}(\boldsymbol{t})|} \quad (4)$$

where ρ_{amp} is the amplification factor, $\ddot{x}_{\boldsymbol{table}}(\boldsymbol{t})$ are the soil surface and table accelerations, respectively.

Hysteretic stress–strain loops are usually derived from the measurement of the response at accelerometers to study the non-linear behaviour of selected sand [17]. Moreover, this procedure is summarised by [14]. If the soil is idealised as a one-dimensional shear beam, the shear stresses and shear strains at a particular depth can be calculated by utilising the acceleration measurements at these levels. By integrating the equation of motion using stress-free surface boundary condition, the shear stress at depth z is

TABLE II
Experimental Tests

Test No.	Type of loading	Purpose	Peak amplitude (g)
Exp- 1	Harmonic sine wave	To examine the container boundary wall effect	0.1 g
Exp- 2	Harmonic sine wave	To examine the container boundary wall effect	0.1 g
Exp- 3	Harmonic sine wave	To examine the container boundary wall effect	0.1 g
Exp- 4	Harmonic sine wave	To examine the container boundary wall effect	0.1 g
Exp- 5	Harmonic sine wave	To examine the container boundary wall effect	0.1 g
Exp- 6	Harmonic sine wave	To examine the container boundary wall effect	0.1 g
Exp- 7	Harmonic sine wave	To examine the container boundary wall effect	0.1 g
Exp- 8	Earthquake time history	To investigate the hysteric soil behaviour	0.05 g
Exp- 9	Earthquake time history	To investigate the hysteric soil behaviour	0.1 g
Exp- 10	Earthquake time history	To investigate the hysteric soil behaviour	0.15 g
Exp- 11	Earthquake time history	To investigate the hysteric soil behaviour	0.2 g

g = 9.8 meter(m) / second (s) , kN = kilonewton.

$$\tau(z,t)=\int_0^z \rho\, \ddot{u}\, dz \quad (5)$$

where τ is the shear stress, $\ddot{u}$ is the acceleration, and ρ is the mass density. Using linear interpolation between the acceleration measurements at different depths (e.g. ACC1, ACC6 and ACC7), the discrete shear stress value at depth z is:

$$\tau_i(t)=\sum_{k=1}^{i=1} \rho \frac{\ddot{u}_k+\ddot{u}_{k+1}}{2} \Delta z_k \quad i=2,3\ldots \quad (6)$$

where subscript i refers to the depth z_i in Fig. 6 (a), $\tau_i = \tau(z_i,t)$: $\ddot{u}_i$=u(z_i, t) and Δz_k is the soil slice thickness.

The corresponding shear strain value γ_i can then be calculated [11]. The displacement values are derived from the double integration of the acceleration time-histories iz.

$$\gamma_i = \frac{1}{\Delta z_{i-1}+\Delta z_i}\left[(u_{i+1}-u_i\frac{\Delta z_{i-1}}{\Delta z_i}+u_{i+1}-u_i\frac{\Delta z_i}{\Delta z_{i-1}}\right] \quad (7)$$

Equations (6) and (7) depend on the surface acceleration measurement. In practice, it was difficult to determine since the accelerometers should keep in good contact with the soil particles. Moreover, reliable acceleration measurement within the shear stack sample's uppermost horizons is complicated by the discontinuity of the significant stiffness between the lightly stressed sand and the embedded instrumentation.

It is well known that sand can have volumetric change when it shears. For the medium-dense soil, seismic excitation makes a net contraction of the deposit evidenced as settlement of the sample surface. The test soil void ratio of soil decreased when the soil density increased. These variations should be reflected

in the calculations for stiffness and shear stress. For the adopted soil in question, measured contractions had a negligible effect on other parameters, and the volumetric change was insignificant.

We investigate a linear relation for the accelerations recorded at the soil base and surface.

$$\ddot{u}_{d=0}(t)= \ddot{u}_{d=H}(t)+H(\ddot{u}_{z=0.550}(t)-\ddot{u}_{d=H}(t))/0.550 \quad (8)$$

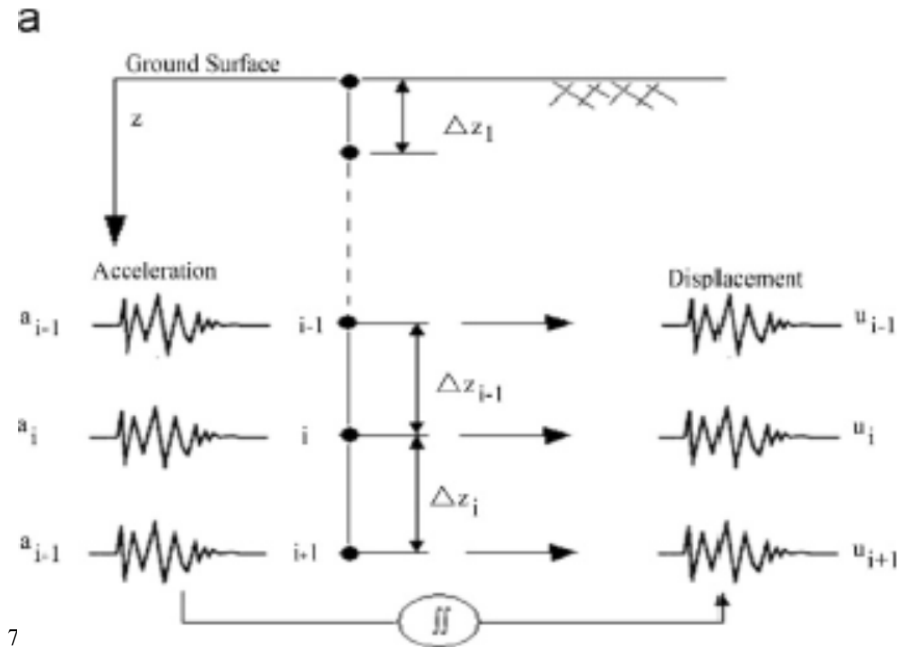

Fig. 6 Accelerometer array and soil discretization for use in stress–strain calculations

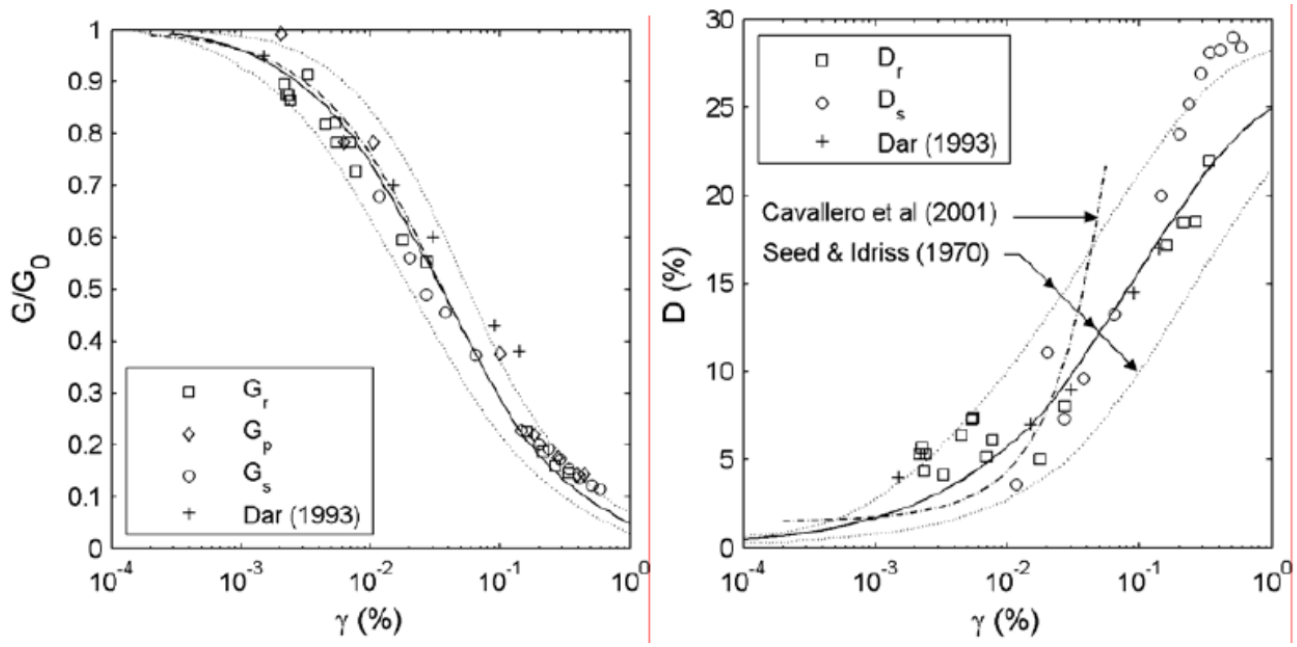

(a) (b)

Fig. 7 (a) The evolution of shear modulus G with shear strain γ (b) The evolution of damping ratio D with shear strain γ [12]

VII. Evaluation of Soil Dynamic Behavior

The literature [4] presents three techniques for estimating the shear modulus G and damping D of soil containers on shaking table. Each of them makes use of a different horizontal excitation waveform which is random, pulse, and sine dwell excitation. Reference [4] adopted the frequency response functions derived from random excitation tests to extract the dynamic soil properties. Reference [4] directly measured shear wave travel times during tests but stopped short of calculating shear moduli from the interpreted

velocities. Reference [1] determined the dynamic soil properties via a geometric analysis of the hysteretic response recorded in the centrifuge by using a sinusoidal type excitation.

Data are evaluated by comparison of the two datasets of charts[12], [18], [6], [15] which are the evolution of G / G0 and Damping with strain level, see Fig. 8.

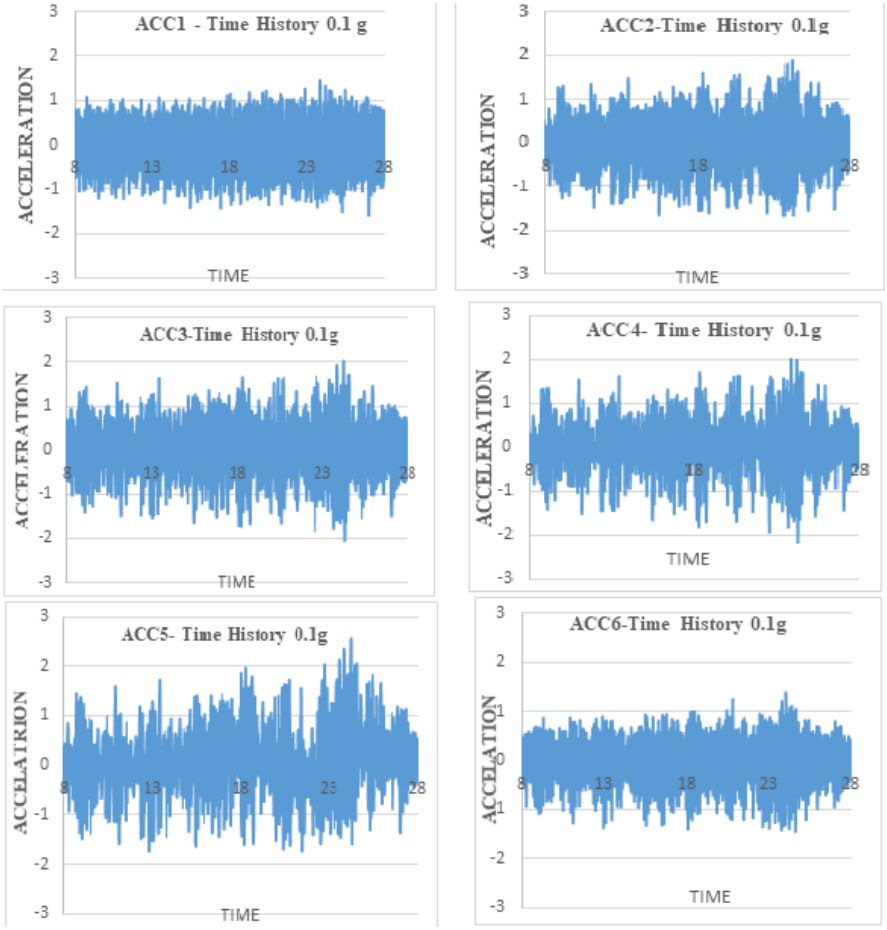

Fig. 8 The influence of the container boundaries on the dynamic soil response (Time History waves)

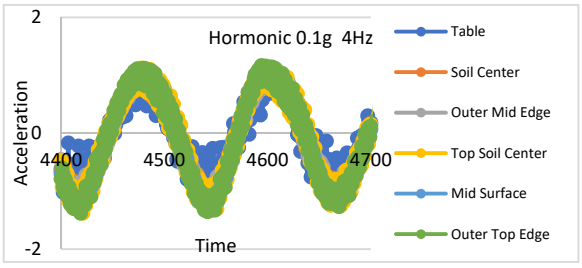

Fig. 9 The effect of the container boundary of the soil

VIII. Assessment of Boundary Effects

Fig. 9 shows the acceleration time histories at ACC1-ACC6 in Exp 7 and Exp 9. The results show that the differences among the responses at ACC1-ACC6 were insignificant. The response of ACC5 and ACC6 was situated on the container outer boundary, and it showed a scattered shape. However, the peak amplitude remained around 0.1 g, which was very close to peak amplitudes measured by other six accelerometers of Exp 7 test. These results demonstrate that the flexible boundaries of the soil container functioned appropriately. The scattered shape at ACC5 and ACC6 can be considered with limited local effect on an area close to the wall container only.

From the above approximations, the shear modulus and damping ratio of the soil were calculated from the shear stress–strain loops. The soil shear modulus using the secant slope and the damping ratio was calculated using the area of the corresponding shear stress–strain loop, see Fig. 8.

The τ'_{zy} and γ_{zy} have, a limiting value. [1] found the set of equations which give the best representative values of Gs and Ds in addition to the equations of τ'_{zy} and γ_{zy}

$$D_s=\frac{1}{4\pi}*\frac{\oint \tau'_{zy}d\gamma_{zy}}{(\tau'_{max}-\tau'_{min})(\gamma_{max}-\gamma_{min})/8} \quad (9)$$

$$G_s=\frac{(\tau'_{max}-\tau'_{min})}{(\gamma_{max}-\gamma_{min})} \quad (10)$$

$$\tau'_{zy}=\boldsymbol{\rho}\mathrm{d}(\ddot{u}_d(\mathrm{t})+(\ddot{u}_{d=0}(\mathrm{t}))/2 \quad (11)$$

$$\gamma_{zy}=(u_d(\mathrm{t})-u_{d=0}(\mathrm{t}))/\mathrm{d} \quad (12)$$

IX. Discussion

For the adopted soil in question, the measured contractions had a negligible effect on other parameters, and the volumetric change was insignificant.

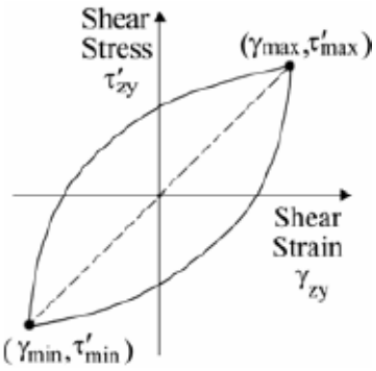

Fig. 10 Dynamic response (harmonic wave)

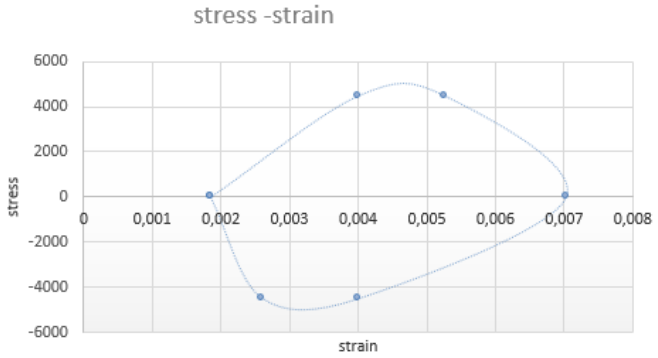

Fig. 11 Stress – strain loop

Fig. 11 shows the stress- strain loop for hysterics soil which is the result of (11) and (12).

Fig. 12 shows how the soil response to different Time history intensity and response increase when the applied input increase

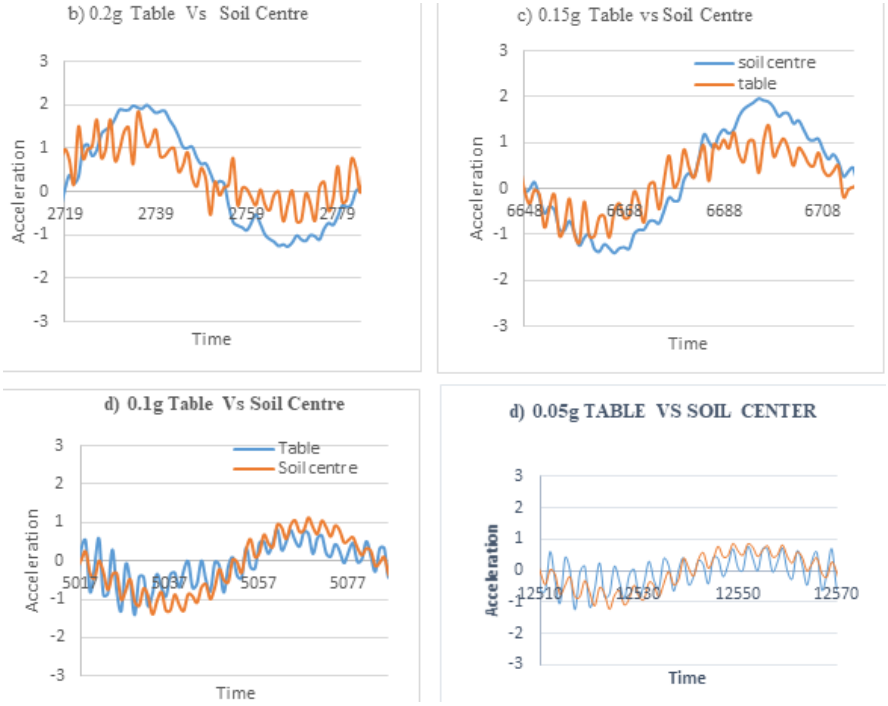

Fig. 12 Soil response

X. Conclusion

The experimental model test is highly recommended in the research of seismic geotechnical problems because of the inadequacy of in situ information. Therefore, a physical model is vital to simulate semi-infinite free-field soil deposit. This paper describes the design and performance of a flexible container, which is based on the base shear limitations of a 1-G shaking table. The performance of the flexible container is evaluated using a series of model tests. The output results show the effect of the boundary on measured accelerations, and these results found the insignificant effect of the soil boundary.

In the past years, many numerical models for modelling the dynamic behaviour of geotechnical problems have been made. Furthermore, sophisticated techniques are now available to tackle the analysis of complex soil structures interaction. However, there is few experimental or prototype information to compare to result against these techniques. Before these techniques are applied in actual, they must be properly validated. The 1/50 scale flexible container developed in this paper can offer an interesting view into the seismic behaviour of large soil specimens.

REFERENCES

[1] Brennan, A. T. N. &. M. S. 2. E. o. s. m. a. d. i. d. c. t. J. o. G. a. G. E. 1. 1.-., 2005. Evaluation of shear modulus and damping in dynamic centrifuge tests. *Journal of Geotechnical and Geoenvironmental Engineering,* pp. 131, 1488-1497.

[2] Chunxia, H. H. Z. G. C. &. Z. S., n. d. Design and Performance of a Large-Scale Soil Laminar Shear Box in Shaking Table.

[3] Clough, R. W. &. P. J., 1975. Dynamics of structures.

[4] Dietz, M. &. M. W. D., 2007. Shaking table evaluation of dynamic soil properties. Proceedings of the 4th International Conference on earthquake geotechnical engineering,

[5] Hardin, B. O. &. D. V. P., 1972. Shear modulus and damping in soils: measurement and parameter effects. Journal of Soil Mechanics & Foundations Div, 98. *Journal of Soil Mechanics & Foundations Div,* p. 98.

[6] Karatzetzou, A. F. S. E. R. K. S. T. G. G. E. P. K. G. N. &. G. G., n. d. A Comparative Study of Elastic and Nonlinear Soil Response Analysis.

[7] Kramer, S. L., 1996. *Geotechnical earthquake engineering, Prentice Hall Upper Saddle River, NJ.*

[8] Meymand, P. J., 1998. Shaking table scale model tests of nonlinear soil-pile-superstructure interaction in soft clay. Issue University of California, Berkeley.

[9] Moss, R. E. C. V. &. K. S., 2010. Shake table testing to quantify the seismic soil-structure interaction of underground structures.

[10] Nielsen, A. H. s., 2006. Absorbing boundary conditions for seismic analysis in ABAQUS. Issue ABAQUS User Conference, pp. 359-376.

[11] Pearson, C. E., 1986. Numerical Methods In Engineering & Science, CRC Press.

[12] Seed, H. B. W. R. T. I. I. &. T. K., 1986. Moduli and Damping factors for dynamic analyses of cohesionless soils. Journal of Geotechnical Engineering, pp. 112, 1016-1032.

[13] Tabatabaiefar, H. R. &. M. A., 2010. A simplified method to determine seismic responses of reinforced concrete moment resisting building frames under the influence of soil–structure interaction. Soil Dynamics and Earthquake Engineering. pp. 30, 1259-1267.

[14] Turan, A. H. S. D. &. E. N. H., 2009. Design and commissioning of a laminar soil container for use on small shaking tables. Soil Dynamics and Earthquake Engineering, pp. 29, 404-414.

[15] Vucetic, M. &. D. R., 1991. Effect of soil plasticity on the cyclic response. Journal of geotechnical engineering, pp. 117, 89-107.

[16] Wolf, J. P. &. O. P., 1985. Non-linear soil-structure-interaction analysis using dynamic stiffness or flexibility of soil in the time domain. Earthquake engineering & structural dynamics. pp. 13, 195-212.

[17] Zeghal, M., n.d. Soil System Identification Using Earthquake Records and Experimental Data.

[18] Zeng, X. &. S. A., 1996, Design and performance of an equivalent-shear-beam container for earthquake centrifuge modelling. Geotechnique. pp. 46, 83-102.

[19] Zhang, C. &. W. J. P., 1998. Dynamic soil-structure interaction: current research in China and Switzerland, Elsevier.